SSRG International Journal of Mechanical Engineering
ISSN: 2348-8360/ https://doi.org/10.14445/23488360/IJME-V13I6P103

Volume 13 Issue 6, 28-34, June 2026

Original Article

Numerical Investigation of Thermo-Mechanical Reliability in Laser- Welded EV Battery Terminal Plate Assemblies

Min-Woo kim[1], Hyeon-Gyo Jeong[1], Hyoung-Woo Lee[2], Dae-Goo Song[3]

[1]*Department of Convergence Engineering, Jungwon University, Republic of Korea.*
[2,3]*Department of Mechanical and Aerospace Engineering, Jungwon University, Republic of Korea.*

[3]*Corresponding Author : song8888@jwu.ac.kr*

Received: 06 March 2026 Revised: 07 April 2026 Accepted: 08 May 2026 Published: 27 June 2026

Abstract *- The terminal components of high-power battery modules for electric vehicles are components that remain mechanically robust while carrying large currents and withstanding welding-induced thermal loads. In this study, a terminal plate assembly made of a 1 mm-thick brass plate with laser-welded studs was selected as the analysis target, and its structural and thermal safety were examined using finite element simulations. Three configurations were considered: a flat base plate, a bent plate without studs, and a bent plate with studs assembled, to clarify the influence of bending geometry and stud attachment on mechanical response and thermal behavior. Under a bending load of approximately four tons, the maximum equivalent stress decreased from 56.17 MPa in the flat plate to 20.11 MPa in the bent plate and further to 18.86 MPa in the stud-assembled model, indicating a clear reinforcement effect of the three-dimensional load path. Transient thermal analysis of laser welding showed peak temperatures of about 1148.1–1153.2°C for simultaneous upper and lower welding, and the difference between the flat and bent geometries was minor because the heat source conditions and boundary constraints were identical. When the temperature field was coupled to the structural analysis, the resulting thermal deformation was limited to roughly 0.25 mm. The average thermal stress ranged between about 28.3 and 39.906 MPa, although localized stress concentration produced much higher maximum values. Considering these numerical results, the terminal plate* assembly *can be regarded as structurally and thermally stable under the assumed loading and process conditions. The analysis framework proposed in this study can serve as a basis for subsequent optimization of terminal geometry and laser welding parameters.*

Keywords *- Electric Vehicle Battery, Terminal plate assembly, Laser welding, Structural analysis, Thermal deformation analysis.*

1. Introduction

With rapidly expanding electrification, the demand for high-power energy systems is increasing in a wide range of applications, including electric vehicles, heavy commercial vehicles, industrial mobility platforms, uninterruptible power supplies, and energy storage systems. As these systems operate under high current and often severe service conditions, the reliability of terminal components and current-carrying joints is an important issue in design.

In practice, the mechanical integrity of a terminal connection cannot be separated from its electrical function, because vibration, fastening force, local heat generation, and repeated operating cycles act simultaneously in actual battery environments. Evaluating the structural safety of terminal joints is therefore an essential step in the design of high-power battery systems [1, 2]. Bipolar lead-acid battery systems have been studied for many years because they and compact and offer advantages in high-power operation. Earlier studies discussed their potential for hybrid electric vehicles and pointed out that the choice of substrate and structural design strongly affects overall performance [3, 4]. It has also been reported that the durability of bipolar structures depends not only on electrochemical behavior, but also on the materials used for current collection, the configuration of the joints, and the quality of the manufacturing process [5].

In battery module manufacturing, the joint quality of busbars, tabs, and terminal interconnects directly affects current transmission performance and durability. In light of this, laser welding processes capable of precise energy control have recently emerged as an important alternative [6, 7]. In particular, laser welding can reduce the heat-affected zone through localized heating and minimize the burden of complex post-processing, and thereby offers strong potential to replace conventional brazing processes [8, 9]. However, the integrity

of an actual welded joint cannot be evaluated solely based on the presence of fusion [13, 14]. For a more rational design assessment, the temperature distribution generated during the process and the resulting thermal stress and thermal deformation should also be considered [10].

In this study, the effects of bending geometry and stud attachment configuration on the structural response of a terminal plate assembly for electric vehicle batteries were first investigated. The thermal behavior and thermo-structural coupled behavior according to laser welding conditions were subsequently evaluated. Through these analyses, the structural and thermal stability of the terminal component were quantitatively examined, and foundational data for future design improvement and process optimization were provided.

In previous studies, tab-to-busbar welding, stud-to-plate welding, and battery pack welding thermal analysis have been performed a lot, but few studies have dealt with structural, thermal, and thermal-mechanical coupled analysis at once at EV battery terminals in the form of "bending terminal plate + stud attachment" [6, 16]. In particular, it is more difficult to find a full transient thermal-mechanical model including a laser welding heat source.

In this study, structural analysis + laser welding thermal analysis, + thermal analysis + thermal-mechanical linkage analysis were performed based on the actual brush terminal plate assembly shape (bending + stud) for EV special vehicles. The effects of bending geometry and stud configuration on stress/deformation and thermal deformation are quantitatively summarized, and initial design guidelines for optimizing future design/welding conditions are to be presented. This study is not just an electrical/thermal analysis, but it directly evaluated the thermal-mechanical reliability of the EV terminal structure.

2. Analysis Target and Methodology

2.1. Analysis Target

The terminal plate assembly analyzed in this study is a current-carrying component applied to high-power battery modules for special-purpose vehicles. The assembly consists of a 1 mm-thick brass conductive plate and two types of studs joined to the upper section. The plate is fabricated through a press bending process, and the studs are connected to the terminal section by laser welding. Because the welded region is simultaneously subjected to concentrated current flow, fastening loads, and thermal loads, it is a critical area for the structural reliability of the product.

The terminal plate is made of brass alloy (C2081), and its properties are similar to the usual α+β brass used in electrical terminals. In the finite element model, an elastic modulus of 100 GPa, a Young's modulus of 115 GPa, and a Poisson rate of 0.345 were used for the brass plate.

Based on representative literature data of brass alloys, the thermal properties were defined as a thermal conductivity of 123 W/m·K, a specific heat of 385 J/kg·K, and a thermal expansion coefficient of 20.8×10^{-6}/K. Room temperature yield strength was measured at 250 MPa by reflecting a brass plate of molding/rolling strength suitable for press-molded battery terminals. The welded brass area has become the most important part in terms of structural reliability under EV battery vibration and clamping loads.

2.2. Structural Analysis Method

As structural analysis was conducted during the initial design stage to evaluate structural safety under mechanical loading conditions. Three configurations were considered in the analysis models: a flat base plate model, a bent plate model without studs, and an assembled model with attached studs. Used ANSYS mechanical APDL 2025 R1 for each model; a bending load of approximately four tons was applied to compare the stress distribution and deformation behavior. Through this approach, changes in the load transfer path according to the bending geometry and stud attachment were evaluated.

All models were discretized using three-dimensional solid elements to accurately capture the structural response under bending conditions. Based on their geometric complexity, a structured and unstructured hybrid mesh strategy was adopted, with a typical element size of approximately 2-5 mm in the region of interest, with sufficient stress gradients resolved. The load was converted to an equivalent force, applying a dispersion pressure to the specified load surface. The load was applied perpendicular to the surface to represent realistic bending conditions.

The boundary conditions were defined to represent the actual mounting and constraints of the structure. Specifically, the object was designed to fold under a force, and was interpreted by fixing the non-folding parts. The folded areas do not significantly affect subsequent processes after deformation. However, the upper parts used in practical operation are welded with studs, which play an important structural role. Therefore, they were fixed to the analysis to accurately represent the actual boundary conditions.

To ensure the reliability of the numerical results, mesh convergence studies have been conducted [13]. Three different mesh densities (sharp, medium, and fine) have been tested, and the resulting maximum stress values have been compared. Variations between the intermediate and fine mesh results have been shown to be within a few percent, confirming that the chosen mesh density provides a good balance between computational efficiency and accuracy.

2.3. Thermal and Thermo-Mechanical Analysis Method

In the laser welding thermal analysis, a 0.2 mm mesh was applied around the weld region to calculate the temperature

gradient more accurately, whereas a 1.0 mm mesh was applied to the remaining regions. For the transient heat transfer analysis, the time increments were set to an initial time step of 0.002 s, a minimum time step of 0.0005 s, and a maximum time step of 0.01 s.

In addition, to reflect the effect of the moving heat source, the welding path was divided into 32 segments, and heat flux was sequentially applied to each segment. The total welding time was set to 10 s, and a convection boundary condition at 22°C was applied to the entire surface to account for heat exchange with air.

To simulate the local concentrated heat source that appears in the laser welding process, the surface heat flux model of this shape was applied. The effective heat input was calculated in consideration of the laser output and the reflection characteristics of the brass material, and the material absorption rate was assumed to be 0.4, to reflect the high reflectance of brass [17].

Accordingly, the heat flux per unit area assigned to each segment was calculated in the relationship of "laser output × absorption rate / corresponding face area". The welding speed and laser spot size were set based on the actual process conditions, and the heat source application time for each segment was adjusted so that the total welding time became 10 s, and at this time, the line energy per unit length was like the range used in the actual process.

Through this moving heat source model and heat input conditions, the temperature history and the size of the Heat-Affected Part (HAZ) predicted in the analysis were set to reasonably approximate the thermal behavior of the actual laser stud welding process.

In the thermal deformation analysis, the temperature field obtained from the thermal analysis was coupled to the structural analysis to evaluate the stress and deformation generated solely by thermal expansion and constraint conditions without external mechanical loading. Fixed support conditions were applied to the rear surface of the plate or fastening hole regions to simulate the actual assembly condition.

Thermal-structural behavior analysis was performed in a sequentially coupled manner. First, the temperature field in the entire welding and cooling process was calculated through the abnormal heat transfer analysis over time, and the temperature distribution obtained in each time step was transferred as the load conditions of the structural analysis to evaluate the stress and deformation caused by thermal expansion.

In the structural analysis, the difference in structural behavior according to the stud welding position and bending shape was compared by calculating the thermal stress and residual deformation that may occur under the constraint conditions after welding based on the results of the thermal analysis.

In this study, direct verification with the experimental temperature measurement and deformation measurement results has not yet been performed, but it was confirmed that the results of a range qualitatively similar to the temperature distribution and melting area size reported in the existing literature on the laser welding heat source model are shown [18, 19].

In the future, we plan to systematically verify the validity of the analysis model through thermal image measurement, observation of the cross-section of the molten part, and quantitative comparison with the results of deformation measurement after welding.

3. Results and Discussion

3.1. Structural Analysis Results

Under the applied bending load of approximately four tons, the three plate configurations showed clearly different stress responses. In the flat base plate model, the maximum equivalent stress reached 56.17 MPa. This case also produced the largest deformation among the three models. When the plate was bent without studs, the maximum stress dropped to 20.11 MPa, and the stud-attached bent plate further reduced the peak stress to 18.86 MPa.

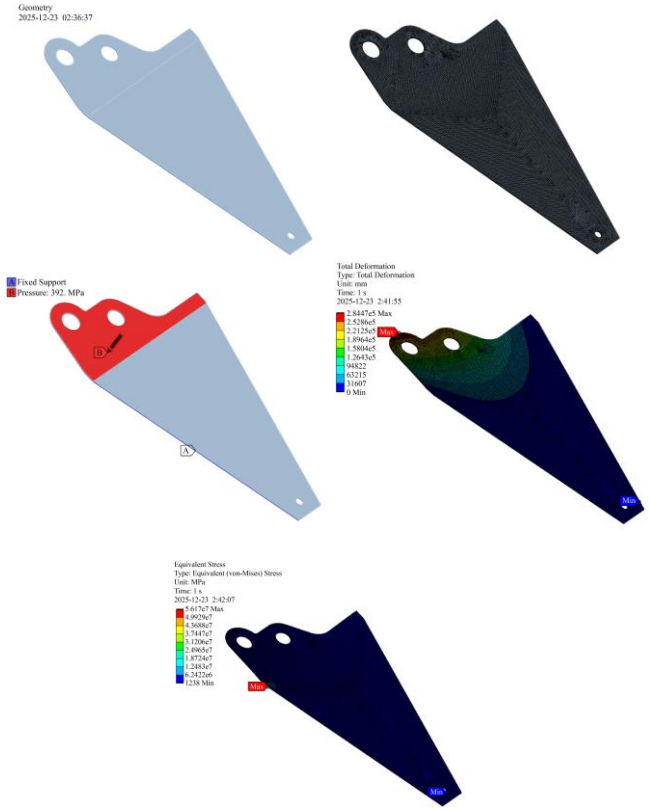

Fig. 1 Base plate structural analysis

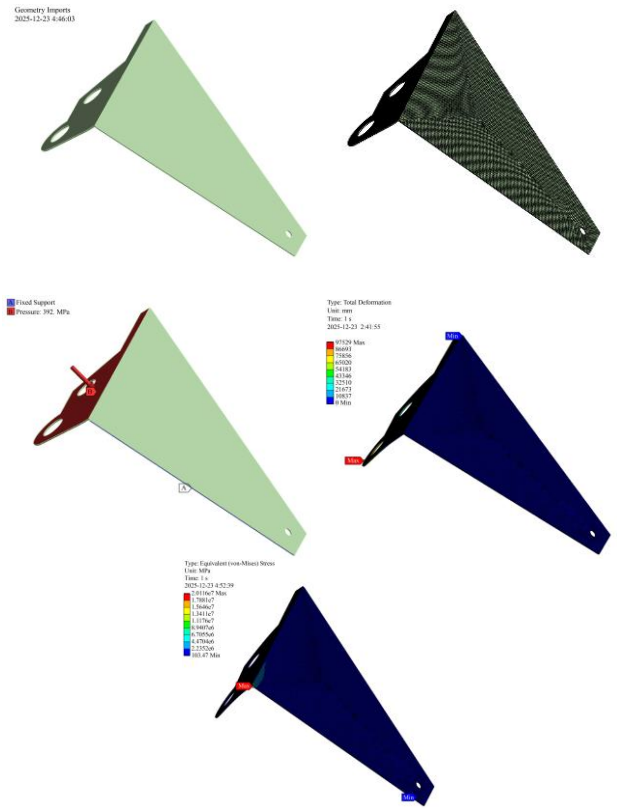

Fig. 2 Bent plate structural analysis

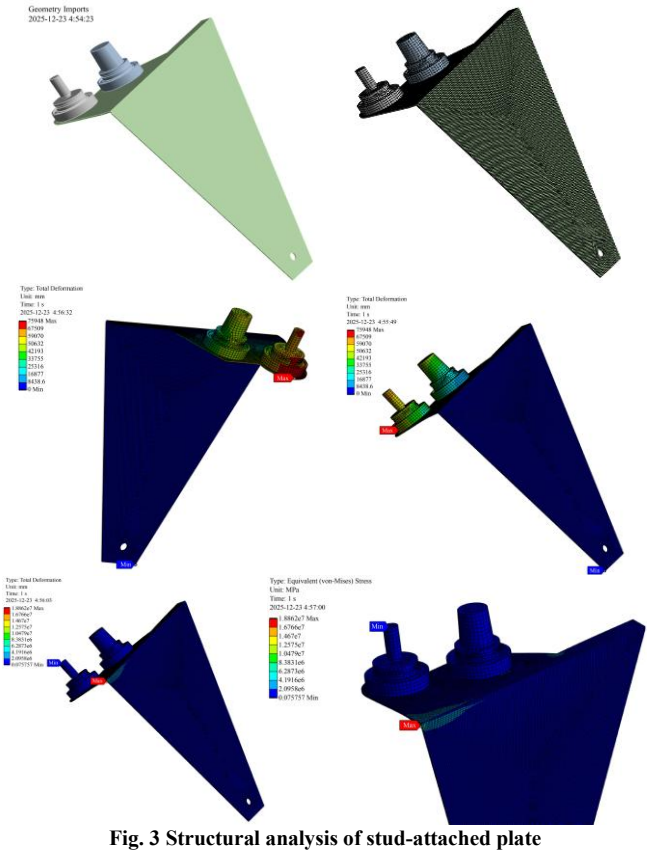

Fig. 3 Structural analysis of stud-attached plate

Table 1. Stress & deformation value for structural analysis of plate

	Base plate	Bent plate	Stud-attached plate
Maximum stress (MPa)	56.17	20.11	18.86
Deformation value	28.44	97.529	75.948

Although the deformation values in the original dataset were reported together with stress units, which requires clarification of the exact unit settings in the analysis software, the relative trend is consistent. The bent and stud-assembled plates showed a structurally more favorable response because the bending geometry and stud attachment increase the second moment of area and allow the external load to be transferred along a three-dimensional path rather than through a simple flat plate. Introducing the bent shape and studs thus effectively enhances stiffness and reduces the concentration of bending stress in the terminal region.

The stress value vs. the material yield strength is below the brace field strength range (250 MPa) suggested in 2.1, and it is safe at a maximum of 56 MPa or 18–20 MPa. Due to the visualization scale factor applied in the post-processing process, the displacement unit notation was different from the actual value in the initial results, and the value in Table 1 reflects the actual displacement (mm) without the scale factor.

3.2. Thermal Analysis Results

In the transient thermal simulations of the laser welding process, the highest temperatures were obtained when the upper and lower sides of the stud were welded at the same time. Under this simultaneous welding condition, both the bent plate model and the flat base plate model exhibited peak temperatures of approximately 1150°C in the weld region. When the upper and lower welds were applied separately, the maximum temperatures were lower than in the simultaneous welding case for both geometries.

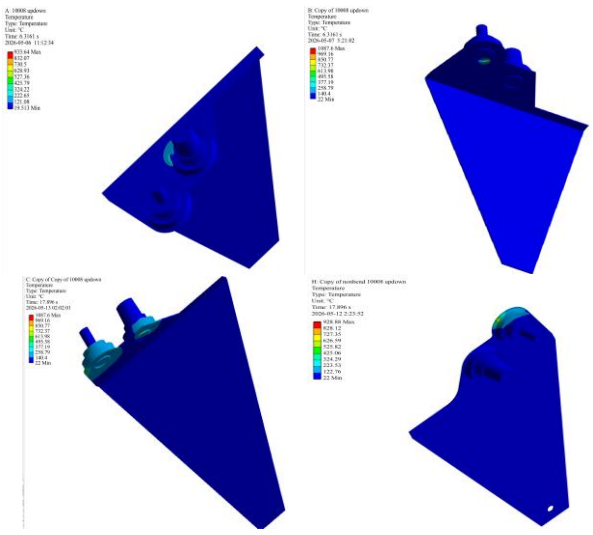

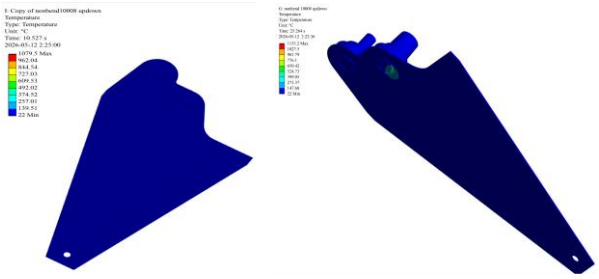

Fig. 4 Thermal analysis of stud-attached plate

Table 2. Difference in plate welding temperature

(°C)	Upper welding	Lower welding	Upper and lower welding
Peak temperature of the bent plate	933.64	1087.6	1148.1
Peak temperature of the baseplate	928.88	1079.5	1153.2

The detailed results show that the peak temperatures for the bent plate and the flat base plate differed only slightly for each welding condition, because the same heat input, material properties, thickness, and boundary conditions were used. This indicates that, for the present configuration, the local peak temperature distribution is governed mainly by the heat source characteristics and the welding path rather than by the difference between the flat and bent plate shapes [20]. Consequently, optimization of the welding process should be focused on parameters such as heat input, irradiation location, and welding sequence, in addition to any geometric modifications of the terminal plate. [11]. It has been reported that the solid-state temperature range of brass begins to melt at about 900-940∘C depending on the composition, and reaches complete melting at 1000-1050°C. The maximum temperature predicted in this study 1150°C-1150°C, exceeds this range, suggesting that local complete melting is possible. However, in the actual welding process, the thermal gradient and cooling conditions are different, so some regions reach above the liquid-state line, while adjacent regions coexist with partial melting located between the solid-state phases. In addition, the result that the peak temperature difference between the plate and the curved shape is insignificant is interpreted to be more sensitive to process variables than to the plate shape, as the thermal reaction is dominated by heat input, welding path, and cooling conditions rather than the shape effect.

3.3. Thermo-Mechanical Analysis Results

When the temperature fields obtained from the welding simulations were mapped onto the structural model, the resulting thermo-mechanical analysis showed that the overall thermal deformation of the plate remained small. The maximum total deformation of the entire structure lay in a narrow range of about 0.245–0.271 mm. This indicates that the terminal plate does not undergo large shape changes under the assumed thermal loading conditions. The average thermal stress levels were also moderate. The bent plate model exhibited an average thermal stress of 39.906 MPa, while the flat base plate under plate-deformation conditions showed a similar value of 39.188 MPa. For the flat plate in the lower-weld deformation case, the average thermal stress decreased to 28.3 MPa.

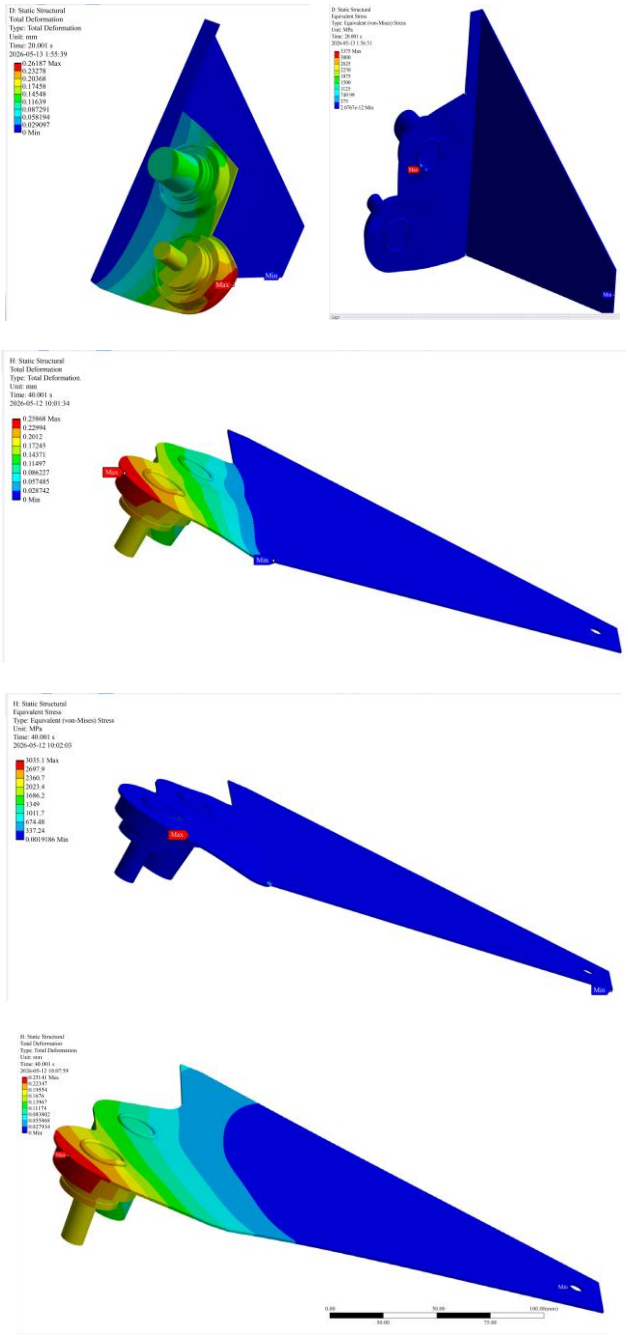

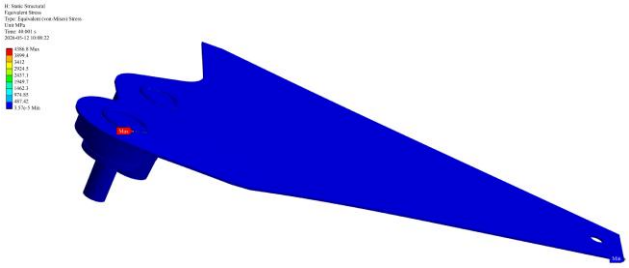

Fig. 5 Thermo-Mechanical analysis of plate

Table 3. Thermal deformation of the plate

	Maximum alue (Mpa)	Average stress (MPa)
Bent plate	33.75	39.906
Base plate (plate deformation)	30.351	39.188
Base plate (lower weld deformation)	43.868	28.3

On the other hand, the calculated maximum stresses for several cases were much higher, ranging from roughly 30.351 to 43.868 MPa. They are therefore interpreted as localized stress concentrations rather than as indicators of overall structural failure. For this reason, the assessment of thermal deformation behavior should not rely only on maximum stress values. For a more appropriate evaluation, the average stress, the magnitude of deformation, and the spatial distribution of stress concentrations together. Under the analysis conditions adopted in this study, the likelihood of excessive global deformation or loss of structural integrity due to thermal loading is judged to be low, and the thermo-mechanical stability of the assembly is generally maintained. [12]. The unit notation was different from the actual value due to the visualization scale factor applied during the thermal analysis post-processing process, and the value reflects the actual displacement without the scale factor.

4. Conclusion

This work numerically investigated the mechanical and thermal behavior of a terminal plate assembly for electric-vehicle battery modules through combined structural, thermal, and thermo-mechanical finite element analyses. The analysis focused on how bending the brass plate and attaching laser-welded studs modify the load-carrying mechanism and the response to welding-induced heat input.

From the structural simulations under a bending load of about four tons, the flat base plate showed the largest equivalent stress, whereas the bent plate and the stud-assembled configuration both exhibited markedly lower stress levels. This trend confirms that introducing bending geometry and studs increases the effective stiffness and redistributes the load path, and thereby improves resistance to deformation.

The transient thermal analysis of the laser welding process revealed that the highest temperature occurred when the upper and lower welds were applied simultaneously. Furthermore, both the flat and bent plate models reached peak temperatures of approximately 1150°C under these conditions. Given that the heat source, material properties, and boundary conditions were identical, the geometric difference between the two plates had only a minor influence on the peak temperature in the weld region.

When the computed temperature fields were mapped onto the structural model, the resulting thermo-mechanical analysis showed that the overall thermal deformation was limited to roughly 0.25 mm and that the average thermal stress ranged between approximately 28 and 40 MPa. Although very high local maximum stresses appeared near geometric discontinuities and constraint regions, these were interpreted as localized concentration effects rather than as indicators of global structural failure.

Taken together, these findings suggest that the investigated terminal plate assembly maintains sufficient structural and thermal stability under the assumed mechanical loading and welding conditions. The analysis procedure established in this study can therefore be used as a reference for refining terminal geometry and selecting appropriate laser welding parameters in future design optimization and experimental validation.

The results of this study provide qualitative guidelines for the selection of major process variables when designing bent/stud terminal plate assembly. In particular, the bending angle should be set within a range that does not induce excessive local stress concentration by considering structural stiffness and thermal deformation sensitivity at the same time, and it is desirable to arrange the stud arrangement in a balanced manner to minimize asymmetry of heat inflow. In addition, the welding sequence is a key factor controlling the heat accumulation and deformation path, and by adopting a stepwise and symmetrical order, the final deformation and residual stress can be effectively reduced.

However, since this study is based on a quasi-static analysis assuming elastic behaviour and a single welding cycle condition, it did not sufficiently reflect various nonlinear and time-dependent phenomena that may occur in the actual process. In particular, factors such as passive stress relaxation, accumulated effects due to repetitive heat loads, material fatigue behaviour, and possible pores and cracks in the actual welding process were not considered. Therefore, this result is valid for identifying qualitative trends, but additional verification is required to be used as a quantitative design criterion.

In future studies, it is planned to secure the reliability of the analysis results through experimental verification using

thermal imaging cameras, strain gauge measurements, and microstructure analysis. In addition, by introducing electric-thermal-mechanical ductility analysis, we intend to expand it to a more sophisticated model, including current density distribution and Joule heating effect. Through this, it aims to more faithfully reflect the actual welding process conditions and improve the deformation and stress prediction accuracy of the terminal plate assembly.

Acknowledgments

This work was supported by the "Chungbuk Automotive Company Leading Technology Research and Development Support Program" (No. 2025-103) conducted by the Chungbuk Institute of Science and Technology Innovation (CBIST), an affiliated organization of Chungcheongbuk-do Province.

References

[1] Jörg Hildebrand, and Hadi Soltanzadeh, "A Review on Assessment of Fatigue Strength in Welded Studs," *International Journal of Steel Structures*, vol. 14, pp. 421-438, 2014. [CrossRef] [Google Scholar] [Publisher Link]

[2] Lee Kyung-hyun, "*A Comparative Study of Residual Stresses and Welding Effect Characteristics Depending on the Welding Method*," Master Thesis, Southern University Graduate School, 2020. [Google Scholar] [Publisher Link]

[3] Michel Saakes et al., "Advanced Bipolar Lead–Acid Battery for Hybrid Electric Vehicles," *Journal of Power Sources*, vol. 95, no. 1-2, pp. 68-78, 2001. [CrossRef] [Google Scholar] [Publisher Link]

[4] Michel Saakes et al., "Development and Testing of a Bipolar Lead-Acid Battery for Hybrid Electric Vehicles," *Journal of Power Source*, vol. 78, no. 1-2, pp. 199-203, 1999. [CrossRef] [Google Scholar] [Publisher Link]

[5] Sunil K. Pradhan, and Basab Chakraborty, "Substrate Materials and Novel Designs for Bipolar Lead-Acid Batteries: A Review," *Journal of Energy Storage*, vol. 32, 2020. [CrossRef] [Google Scholar] [Publisher Link]

[6] Nikhil Kumar, Iain Masters, and Abhishek Das, "In-Depth Evaluation of Laser-Welded Similar and Dissimilar Material Tab-to-Busbar Electrical Interconnects for Electric Vehicle Battery Pack," *Journal of Manufacturing Processes*, vol. 70, pp. 78-96, 2021. [CrossRef] [Google Scholar] [Publisher Link]

[7] Shivam Dave, "*Bimetallic Materials Welding and Analysis for Battery Packs of Electric Vehicles*," Master Thesis, LUT University, pp. 1-89, 2023. [Google Scholar] [Publisher Link]

[8] Jun Soo Park, and Jong Min Kim, "*Finite Element Modelling for Thermal Analysis of Stud-to-plate Laser Brazing for a Dissimilar Metal Joint*," Technical Report, Korea Atomic Energy Research Institute, pp. 1-67, 1996. [Google Scholar] [Publisher Link]

[9] Luis Contreras, Matthew Hoffmeyer, and Zainal Abidin, "Thermal Finite Element Modelling and Prediction of Laser Welded Battery Packs," *WCX SAE World Congress Experience*, Detroit, Michigan, United States, 2026. [CrossRef] [Google Scholar] [Publisher Link]

[10] Nikhil Kumar et al., "Real-Time Electro-Thermo-Mechanical Performance Evaluation of Laser Welded AA 1050 Busbar," *Journal of Energy Storage*, vol. 103, pp. 1-11, 2024. [CrossRef] [Google Scholar] [Publisher Link]

[11] Subin Shin et al., "Laser Thermography Inspection of Weld Defect in Lithium-Ion Battery Cap," *Journal of Energy Storage*, vol. 109, 2025. [CrossRef] [Google Scholar] [Publisher Link]

[12] Choong-Gi Kim, Jae-Woong Kim, Kim-Chul Kim, "Welding Distortion Analysis of a Laser Welded Thin Box Structure," *Journal of Welding and joining*, vol. 25, no. 5, pp.72-77, 2007. [CrossRef] [Google Scholar] [Publisher Link]

[13] Elisabeth Hasz Ophaug, "*Finite Element Modeling of Laser Welding Induced Distortion Due to Initial Residual Stresses*," Master Thesis, Aalborg University, pp. 1-53, 2018. [Publisher Link]

[14] Anton Rolseth, and Anton Gustafsson, "*Implementation of Thermomechanical Laser Welding Simulation: Predicting Displacements of Fusing a AISI 304 T Joint*," Master Thesis, University of Skövde, 2021. [Google Scholar]

[15] Andrew Ko, "*Durability of Aluminum Copper Laser Welds for EV Battery Applications*," Thesis, University of Waterloo, pp. 1-88, 2024. [Google Scholar] [Publisher Link]

[16] Ikuo TANABE, "Development of FEM Thermal Simulation Technique for Laser Keyhole Welding," *Journal of Machine Engineering*, vol. 26, no. 1, pp. 5-18, 2026. [CrossRef] [Google Scholar] [Publisher Link]

[17] Nikhil Kumar et al., "In-Depth Evaluation of Laser Welding of Thick Busbar to 21700 Li-ion Cell Terminal for Electric Supercar Vehicle Battery Pack," *Journal of Manufacturing Processes*, vol. 33, pp. 3058-3067, 2024. [CrossRef] [Google Scholar] [Publisher Link]

[18] Stefan Schaeffler et al., "Experimental Characterization of Thermal Contact Resistances for Laser-Welded Battery Cell Connections using Laser Flash Analysis," *Journal of Energy Storage*, vol. 152, pp. 1-13, 2026. [CrossRef] [Google Scholar] [Publisher Link]

[19] Andreas Andersson Lassila et al., "Effects of Different Laser Welding Parameters on the Joint Quality for Dissimilar Material Joints for Battery Applications," *Optics & Laser Technology*, vol.177, pp. 1-14, 2024. [CrossRef] [Google Scholar] [Publisher Link]

[20] Jarno Saruaho "*Mechanical Load Capacity of Laser Beam Welds in Electric Vehicle Batteries*," Master Thesis, Aalto University, pp. 1-78, 2025. [Google Scholar] [Publisher Link]